RSC Advances

PAPER

View Article Online
View Journal | View Issue

Cite this: *RSC Adv.*, 2024, **14**, 18417

β-Enaminonitrile in the synthesis of tetrahydrobenzo[*b*]thiophene candidates with DFT simulation, *in vitro* antiproliferative assessment, molecular docking, and modeling pharmacokinetics†

Amna S. Elgubbi,[a] Eman A. E. El-Helw,[b] Motaleb S. Abousiksaka,[a] Abdullah Y. A. Alzahrani[c] and Sayed K. Ramadan *[b]

Received 7th May 2024
Accepted 2nd June 2024

DOI: 10.1039/d4ra03363a

rsc.li/rsc-advances

Among sulfur-including heterocycles, the benzothiophene skeleton is one of the worthy structure fragments that exhibit structural similarities with active substrates to develop various potent lead molecules in drug design. Thus, some tetrahydrobenzo[*b*]thiophene candidates were prepared from the β-enaminonitrile scaffold *via* reactions with diverse carbon-centered electrophilic reagents and supported with DFT studies. The *in vitro* antiproliferative effect was screened against MCF7 and HePG2 cancer cell lines, and the results displayed the highest potency of imide **5**, Schiff base **11**, and phthalimido **12** candidates. A molecular docking study was operated to explore the probable binding modes of interaction, and the results revealed the good binding affinity of compounds **5**, **11**, and **12** toward the tubulin protein (PDB ID 5NM5) with respect to paclitaxel (a tubulin inhibitor) and co-crystallized ligand (GTP). Besides, modeling pharmacokinetics analyses displayed their desirable drug-likeness and bioavailability properties.

Introduction

In nature, heterocyclic cores are widely distributed, and many heterocyclic compounds synthesized in laboratories have been utilized as clinical agents.[1–6] The most characteristic and important constituents of living cells, DNA and RNA, contain heterocyclic scaffolds. Sulfur-including heterocycles exhibit various biological properties due to the similarities with many natural and synthetic molecules of known potentials.[7–10] Thus, the sulfur heterocyclic family involves highly stable aromatic compounds which show physicochemical properties with relevance in the design of new materials.[11]

In literature, various thiophene derivatives have been reported as antitumor agents as depicted in Fig. 1.[12–14] In turn, a tetrahydrobenzo[*b*]thiophene core is one of the privileged structures in drug discovery as this core exhibits diverse biological effects allowing them to act as antitumor, anti-inflammatory, antibacterial, and analgesic agents.[15–18] Further, several benzothiophenes, as clinical drugs, have been extensively utilized for treating various types of diseases with high therapeutic potency. Therefore, their structure–activity relationships (SAR) have generated more interest among medicinal chemists, and this has concluded in the discovery of various lead molecules against many diseases.

In particular, 4,5,6,7-tetrahydrobenzo[*b*]thiophene candidates have been recognized as promising anticancer agents.[19] Numerous candidates showed their antiproliferative effects through targeting metalloproteinases 2 and 9 (MMP 2 and 9), HIF-1α and the vascular endothelial growth factor receptor,[20] the epidermal growth factor receptor (EGFR), human EGFR-related receptor 2 (HER2),[21] and the colon cancer-related genes, namely, collagen type X α1 (COL10A1) and collagen type XI α1 (COL11A1) (*cf.* Fig. 2).[22]

On the other side, microtubules, with diverse roles within the cell, are cellular polymers including chromosomal segregation, cytokine, and chemokine secretion, protein trafficking, maintenance of cell structure, cell migration, and division. Therefore, targeting tubulin dynamics is a promising attempt for new chemotherapeutic agents. Substances capable of disturbing microtubules by either stabilizing or destabilizing them would exhibit antiproliferative effects *via* enhancing mitotic arrest and cell apoptosis. At least three main binding sites in tubulin protein, including colchicine, taxane, and vinca

[a]*Chemistry Department, Faculty of Science, Misurata University, 2478, Misurata, Libya*

[b]*Chemistry Department, Faculty of Science, Ain Shams University, Cairo, 11566, Egypt. E-mail: sayed.karam2008@sci.asu.edu.eg*

[c]*Chemistry Department, Faculty of Science and Arts, King Khalid University, Abha, Mohail Assir, Saudi Arabia*

† Electronic supplementary information (ESI) available: Full experimental details, tables, figures, and spectroscopic data. See DOI: https://doi.org/10.1039/d4ra03363a

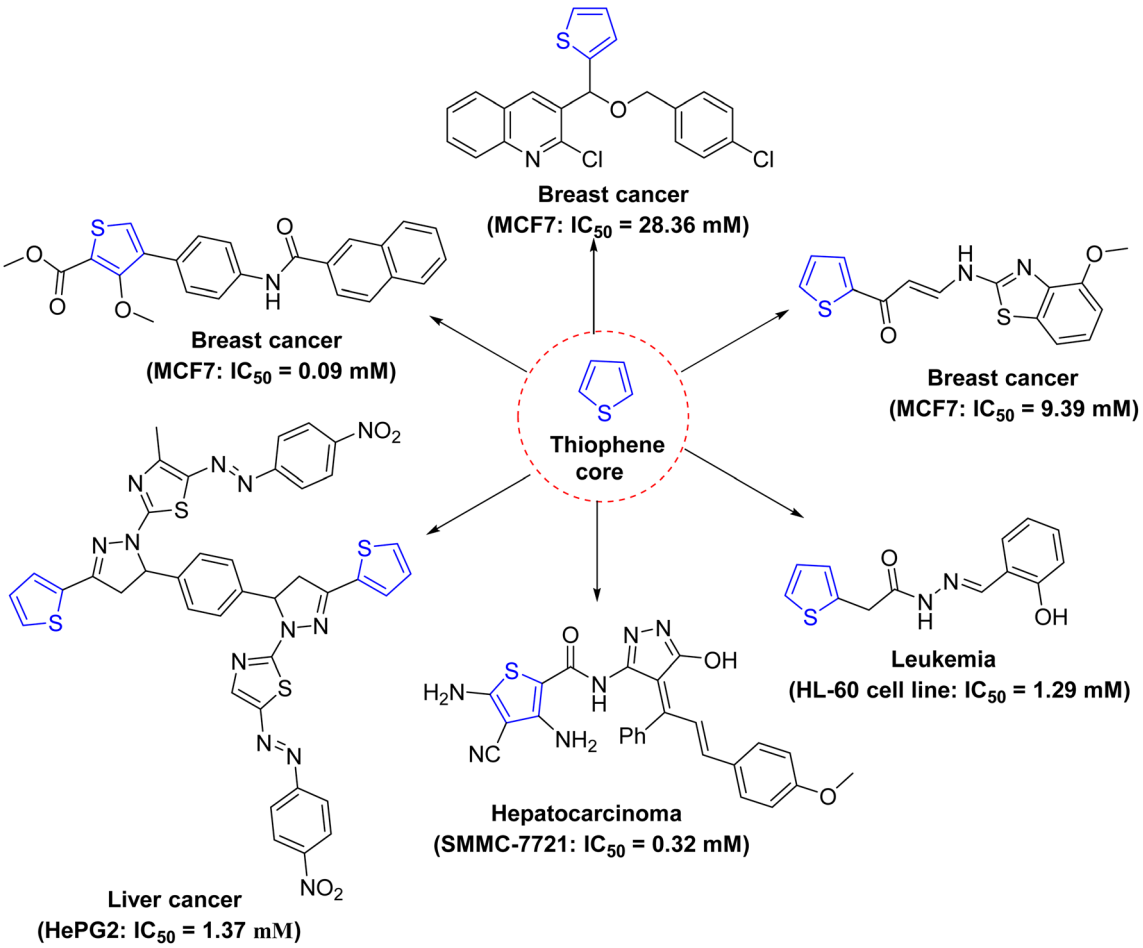

Fig. 1 A diverse thiophene scaffolds as antitumor agents.

alkaloid, have been recognized as targets for the anticancer drugs.[18,23,24]

Therefore, tetrahydrobenzo[*b*]thiophene scaffold was selected as a central heterocyclic motif for the present work and a phenyl ring attached at position-6 to keep its common structural integrity. However, another fused heterocyclic ring or benzene ring connected *via* amide, imide, and imine linker offer various insight with new molecular scaffold resulting in a stronger interaction with key role amino acid residues. These hybrids were an attempt to reach some antitumor agents with potent effect. Continuing our attempts for diverse heterocyclic candidates with pharmaceutical interest,[25–32] this work targeted to design and prepare a new series of tetrahydrobenzo[*b*]thiophenes to evaluate their *in vitro* antiproliferative potency and supported by DFT, molecular docking, and modeling pharmacokinetics studies.

Rationale and design

The rationale of our molecular design was dependent on the generation of two scaffolds of tetrahydrobenzo[*b*]thiophenes. The first one consisted of tetrahydrobenzo[*b*]thiophene moiety with chemical substitutions at position-2 as compounds **2**, **3**, **5**, **6**, **8**, **11**, and **12**. The substitution pattern on the tetrahydrobenzo[*b*]thiophene moiety was chosen to ensure various electronic and lipophilic environments manipulating the potency of the target substrates. The second scaffold consisted of a planar system including tetrahydrobenzo[*b*]thiophene core (chromophore) with pyrimidine skeletons like compounds **4**, **7**, **9**, and **10** (Fig. 2). Also, owing to the reported significant anticancer effects of electron-withdrawing groups, the nitrobenzylidene moiety was selected.[33,34] The two designed scaffolds aimed to include the main pharmacophoric features; the planar polyaromatic system (chromophore) was represented by tetrahydrobenzo[*b*]thiophene core and its side chains or fused rings. Furthermore, most designed substances include basic nitrogen atoms that may be protonated at physiological pH to form cationic centers enhancing the affinity and selectivity of these substances.

Results and discussion

Synthesis

The frequent reactivity modes of bifunctional β-enaminonitriles come from the presence of highly nucleophilic center (NH_2) and electrophilic center (CN). Also, to design and develop new potential antitumor agents, 2-amino-6-phenyltetrahydrobenzo[*b*]thiophene-3-carbonitrile **2** (ref. 35) was prepared through one-pot three components approach *via* interaction of 4-

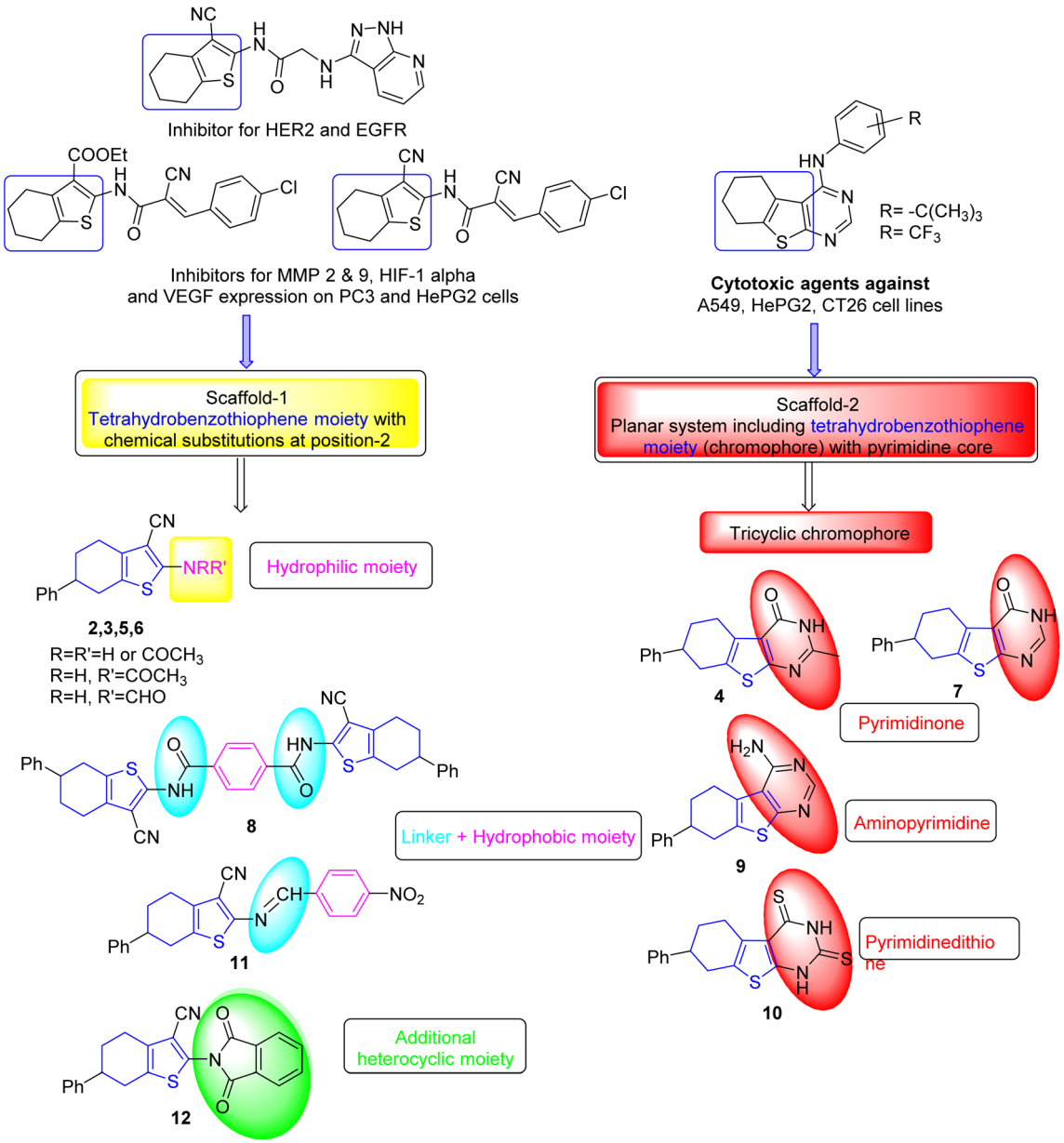

Fig. 2 Examples of certain reported tetrahydrobenzo[*b*]thiophene derivatives as anticancer agents and rationale of molecular design of the chemical structures of the target substrates.

phenylcyclohexanone with malononitrile and elemental sulfur under basic conditions (Scheme 1). Thus, the β-enaminonitrile **2** was allowed to react with diverse carbon-centered electrophiles.

Indeed, treating the enaminonitrile **2** with ethanoic anhydride for 1 or 4 h produced the *N*-acetyl derivative **3** and the heteroannulated product, tetrahydrobenzo[*b*]thienopyrimidine derivative **4**, respectively. In IR of **3**, cyano group was retained and a carbonyl absorption band was detected. While in IR of **4**, the cyano absorption disappeared and a carbonyl absorption band appeared. Their ^{1}H NMR displayed a singlet signal for methyl protons. Moreover, the mass spectrum of **3** furnished peaks at m/z = 296.09 (12%) corresponding to its molecular weight (with molecular formula: $C_{17}H_{16}N_2OS$), m/z = 268.11 (14) corresponding to $[M–CO]^{+\bullet}$, m/z = 229.09 (20%) due to loss of (N≡C–CH=C=O), and the base peak at m/z = 228.07 (100%) corresponding to the elimination of ketene molecule (CH_2=C=O) followed by loss of $^{\bullet}$CN fragment. The ^{13}C NMR of **4** offered signals for carbonyl carbon at δ 163.35 ppm and C=N carbon at δ 158.53 ppm.

Otherwise, conducting **3** with ethanoic anhydride or ethanoic acid glacial/sulfuric acid acquired a mixture of the annulated product **4** and *N*,*N*-diacetyl derivative **5**, which have been separated *via* fractional recrystallization. In the IR chart of imide **5**, NH absorption was absent, and two absorption bands appeared according to vibrational coupling. Its ^{1}H NMR offered singlet signal integrated to six protons at δ 2.34 ppm corresponding to two symmetrical methyl protons.

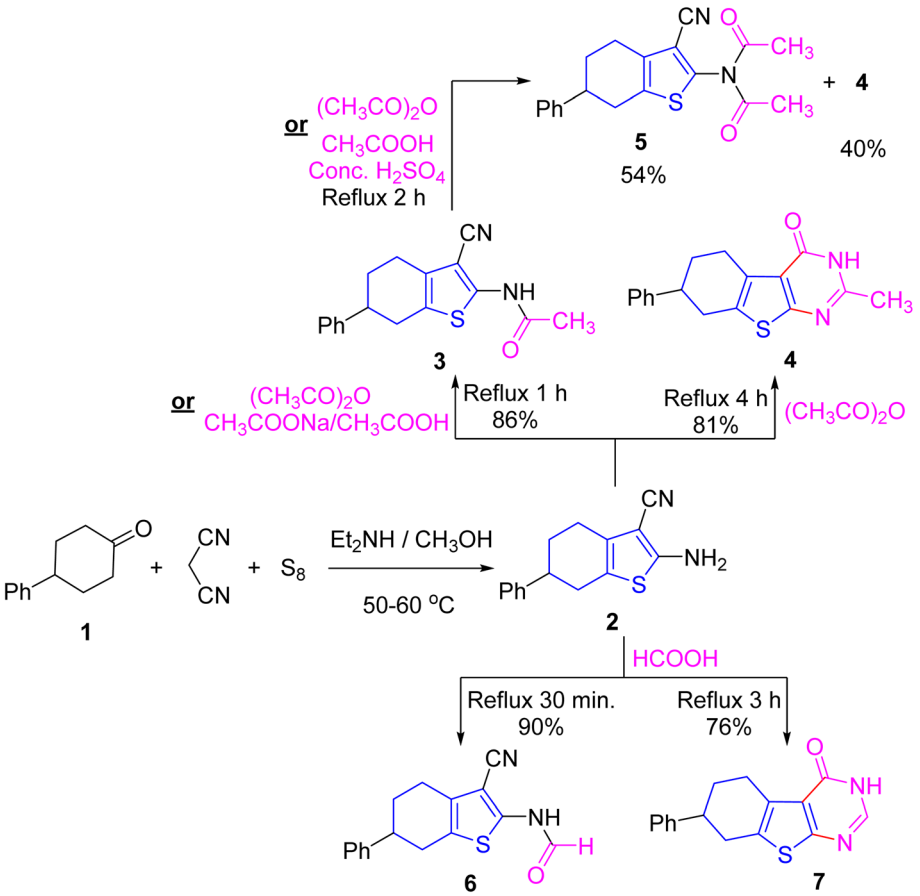

Scheme 1 Synthesis and reactions of **2** with ethanoic anhydride and methanoic acid under diverse conditions.

In turn refluxing **2** with methanoic acid for 30 min and 3 h afforded *N*-formyl derivative **6** and the annulated product **7** as white crystals, respectively (*cf.* Scheme 1). IR of **6** conserved cyano group (ν 2212 cm^{-1}) and displayed NH and C=O absorption bands at ν 3185 and 1684 cm^{-1}, respectively. Whilst IR of **7** was devoid of cyano absorption band but offered absorptions for NH band ν 3190 $cm^{-1}$and C=O at ν 1659 cm^{-1}. Also, ^{1}H NMR of **6** displayed a singlet signal for CHO proton at δ 8.50 ppm and an exchangeable singlet for NH proton at δ 8.67 ppm. In turn, ^{1}H NMR of **7** disclosed singlet signals at δ 8.02 and 12.34 ppm for CH=N and NH protons, respectively.

Stirring a solution of the β-enaminonitrile **2** with terephthaloyl dichloride in a ratio of 2 : 1, respectively, in 1,4-dioxane including triethylamine acquired bis-terephthalamide candidate **8**. In its IR, the amide carbonyl absorption was detected. Also, its ^{1}H NMR disclosed an exchangeable singlet signal for NH proton at δ 11.97 ppm. In turn, refluxing **2** with formamide produced tetrahydrobenzothienopyrimidine derivative **9**. Its IR lacked both carbonyl and nitrile absorptions, but it displayed an absorption for primary amino group at ν 3285, 3200 cm^{-1}, in addition to C=N absorption at ν 1636 cm^{-1}. Further, its ^{1}H NMR offered exchangeable singlet signal for NH_2 protons at δ 6.84 ppm, besides a singlet signal for methine (CH=N) proton at δ 8.20 ppm.

Heating **2** with carbon disulfide in pyridine or alcoholic potassium hydroxide at 60–70 °C led to the construction of tetrahydrobenzothienopyrimidinedithione derivative **10** (*cf.* Scheme 2). In its IR, both primary amino and nitrile groups were disappeared while NH and C=S were detected at ν 3119 and 1190 cm^{-1}, respectively. Also, its ^{13}C NMR displayed signals of C=S groups at δ 181.65 and 169.22 ppm. Further, its ^{1}H NMR detected two NH protons at δ 13.22 and 13.89 ppm.

Perhaps, the utility of pyridine or alcoholic potassium hydroxide were responsible for the existence of thiocarbamate intermediate [**I**] which subsequently attacks the nitrile core *via* 1,6-*exo*–*dig* cyclization to furnish pyrimidine or potassium salt followed by rearrangement to isothiocyanate derivative which underwent 1,6-*exo*–*dig* cyclization and eliminate pyridinium hydrochloride or potassium chloride (*cf.* Scheme 3).

Condensation of enaminonitrile **2** with 4-nitrobenzaldehyde in refluxing ethanoic acid produced the Schiff base candidate **11**. The NH_2 group was absent in its IR and ^{1}H NMR spectra. As for its IR spectrum, C≡N group was conserved (at ν 2218 cm^{-1}), whilst the C=N moiety was detected at ν 1600 cm^{-1}, in addition to the NO_2 functionality was appeared at ν 1556 and 1336 cm^{-1}. As for its ^{1}H NMR, the methine proton (CH=N) appeared at δ 8.84 ppm. Further, its mass spectrum displayed the molecular ion peak at m/z = 387.35 (38%) in addition to other abundant peaks.

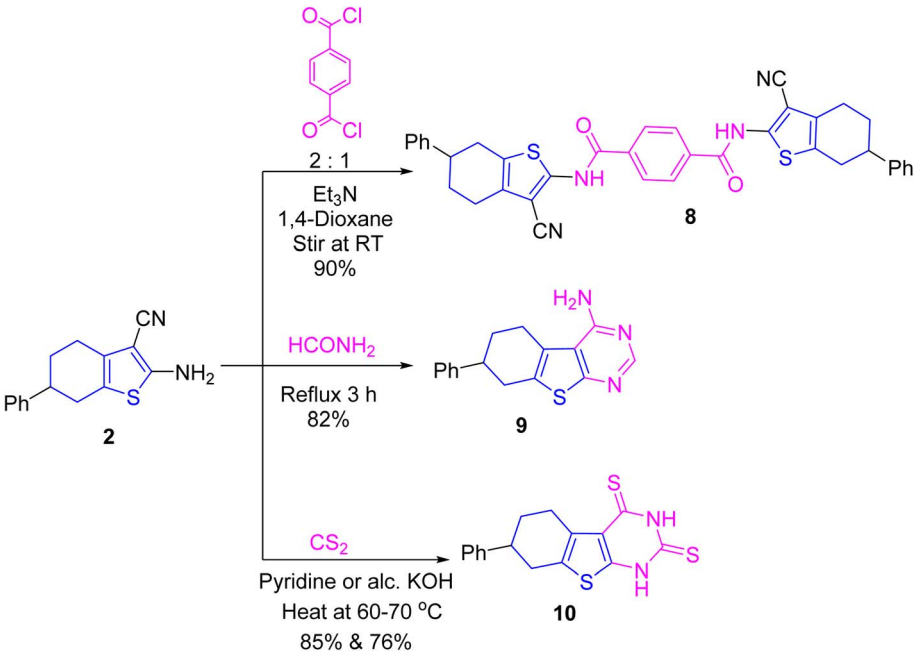

Scheme 2 Reactions of **2** with terephthaloyl dichloride, formamide, and carbon disulfide.

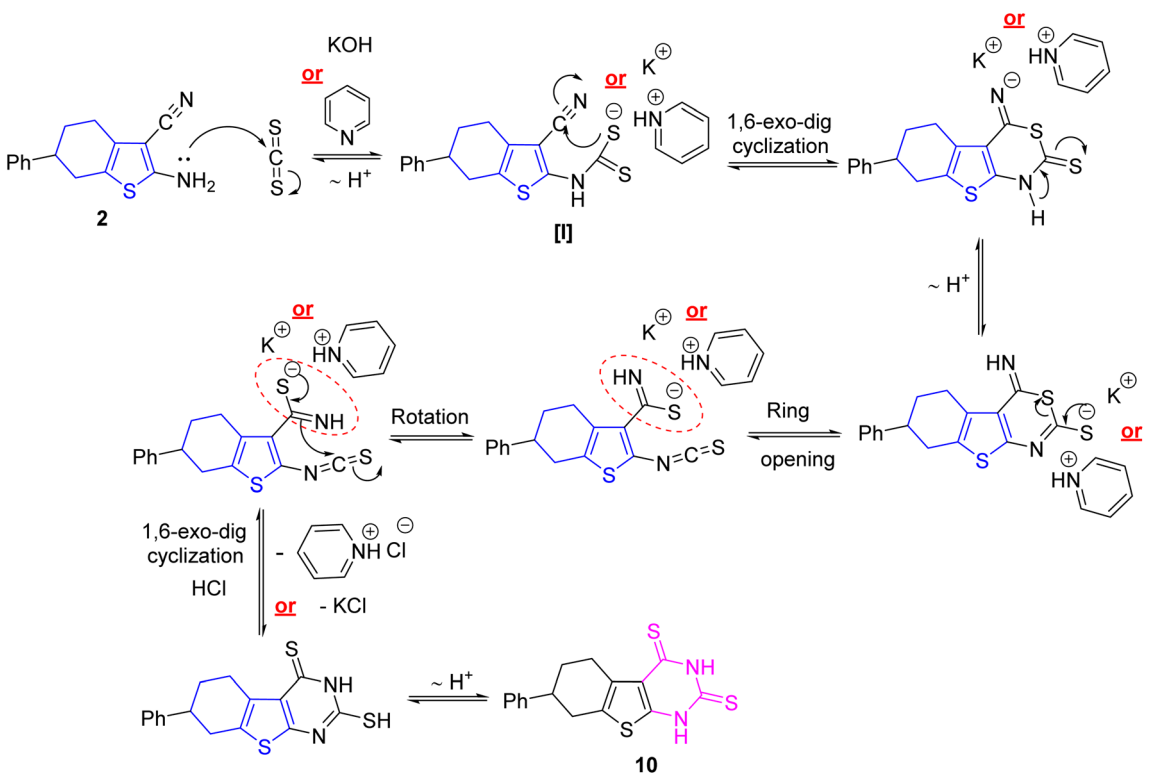

Scheme 3 A suggested pathway for compound **10**.

Treating **2** with phthalic anhydride in refluxing ethanoic acid achieved the phthalimide derivative **12** (*cf.* Scheme 4). In its IR spectrum, the NH_2 moiety disappeared, the nitrile absorption was retained, and the carbonyls of imide linkage were detected at ν 1788 and 1730 cm^{-1} (due to vibrational coupling between symmetrical and asymmetrical stretching absorptions). Further, its mass spectrum offered $M^{+\bullet}$ peak at m/z = 384.31 (22%) and the base at m/z = 77 (100) corresponding to phenyl cation (*cf.* ESI Experimental section†). All methods of synthesis gave the mentioned compounds with different % yields as displayed in schemes and experimental part, without isolation of by-products.

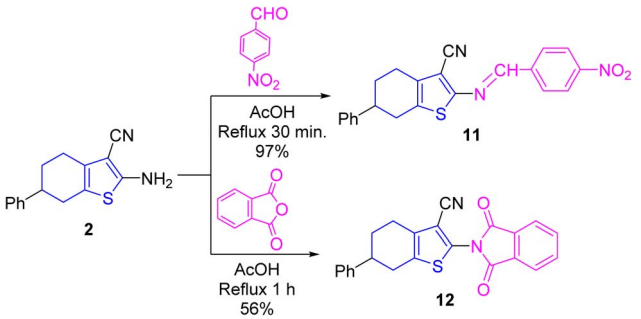

Scheme 4 Reactions of **2** with 4-nitrobenzaldehyde and phthalic anhydride.

DFT (density functional theory) study

The DFT simulation assists in demonstrating the chemical reactions of substrate with various reagents and shows high accuracy for producing of experimental results,[36,37] as well as expecting the appropriate biological applications. DFT simulation was conducted to optimize the molecular structures of the produced substances and identify both nucleophilic and electrophilic centers. The optimization of molecular structures of produced benzo[*b*]thiophene candidates were carried out to create a stable geometry.

The electrophilic-attacking centers are illustrated by HOMO regions of largest electron density (considered as a donor), while the nucleophilic-attacking sites are represented by LUMO areas (considered as an acceptor). The optimized, HOMO, and LUMO structures of substances **2–12** were drawn employing ChemBio3D Ultra 14.0 and portrayed in Fig. S1 (*cf.* ESI†). The HOMOs are dispersed around thiophene unit and LUMOs are focused on benzene moiety. The high E_{HOMO} values are likely to signify a molecule's strong tendency for donating electrons.

To demonstrate how the β-enaminonitrile **2** reacted with some reagents to produce substances **3–12**, DFT simulation was employed to calculate quantum chemical properties including global hardness (η), global softness (ς), chemical potential (μ_o), global electrophilicity index (ω), nucleophilicity index (n), ionization potential (I_P), electron affinity (EA), and electronegativity (x) (*cf.* Table S1 in ESI†). Spectral and analytical data confirmed the assigned structures. The results of parameters calculations were in good agreement with the anticancer efficiency. The lower values of energy gap ($\Delta E = E_{LUMO} - E_{HOMO}$) means low energy needed to remove an electron from the last occupied orbital.[38,39]

Substrates of small ΔE values are mostly referred to as soft compounds, which are more reactive towards radical surface interactions; being efficient of donating electrons easily to hole surface, and therefore might display strong inhibition efficiency. The results showed that energy gap values (ΔE) follow the order: **11** < **12** < doxorubicin < **5** < **9** < **2** < **4** < **7** < **10** < **8** < **6** < **3** (*cf.* Fig. 3). Thus, Schiff base **11** exhibited the lowest ΔE value (1.540 eV) compared to others.

Chemical softness values (σ, eV^{-1}) decrease in the order of **11**, **5**, **12**, **9**, **2**, **4** = **7**, **10**, **3**, **8**, and **6**, respectively (*cf.* Fig. 3), while the hardness values rise in the same order. That is, lower values of softness and higher chemical hardness establish a good stability of the *N*-formyl derivative **6** which might exhibit high molecular hardness. According to the ionization potential (I_P) values of these compounds, the acetamide derivative **3** exhibited the highest I_P value (8.164 eV) which means that it is more difficult to remove an electron from its HOMO orbitals. Besides, the *N*,*N*-diacetyl derivative **5** showed the lowest electron affinity (1.975 eV) indicating the highest molecular reactivity to nucleophiles. The dipole moments showed that Schiff base **11** exhibited the highest value (3.458 debye) which indicates stronger intermolecular interaction than other compounds and interacting more with the surrounding environment.

The scavenging ability toward positive hole, radical, tumor, and oxygen removable not only depend upon E_{HOMO} values but

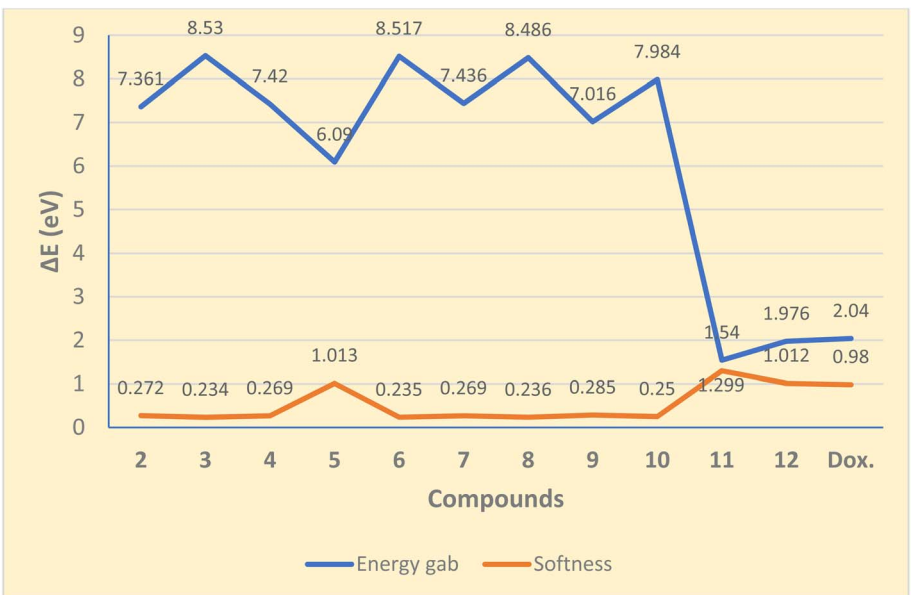

Fig. 3 Energy gap (ΔE, eV) and softness (ς, eV^{-1}) values of the synthesized compounds and doxorubicin.

also, the surface area, number of heteroatoms, electron distributions, and lipophilicity should be considered.[40] The results for most potent compounds encompassing hydrophobic moieties were agreed to an outstanding correlation with oxidation inhibition efficiencies. Compatibly, substrates of higher binding energy showed higher potency due to strong interaction with the receptors' active sites.

Cytotoxic activity assessment

The cytotoxic activity of the substrates was examined against mammary gland breast carcinoma (MCF7) and hepatocellular cancer (HePG2) cell lines utilizing MTT assay and expressed in IC_{50} (growth inhibitory concentration) compared with the untreated controls.[41] The findings indicated variable degrees of inhibitory effect ranged from 71.21 to 9.54 μM by these substrates (Table 1). As for MCF7, the relative highest potency was provided by substances **5** ($IC_{50} = 11.42 \pm 1.4$ μM), **11** ($IC_{50} = 12.93 \pm 1.5$ μM), and **12** ($IC_{50} = 20.51 \pm 2.3$ μM), respectively in comparison to doxorubicin and paclitaxel[42] as reference agents. As for HePG2, the highest potency was furnished by substrates **11** ($IC_{50} = 9.54 \pm 0.7$ μM), **5** ($IC_{50} = 13.73 \pm 1.4$ μM), and **12** ($IC_{50} = 18.16 \pm 1.1$ μM), respectively. Meanwhile, other substrates offered moderate and weak potencies.

Table 1 Cytotoxic activity (IC_{50}, μM) of the tested substrates against MCF7 and HePG2 cell lines with respect to doxorubicin and paclitaxel

	In vitro cytotoxicity: IC_{50}[a,b] (μM)	
Compds	MCF7	HePG2
Doxorubicin	4.50 ± 0.3	4.17 ± 0.2
Paclitaxel[c]	2.50 ± 0.2	4.00 ± 0.3
3	65.20 ± 4.0	71.21 ± 3.5
4	43.21 ± 4.2	50.22 ± 3.9
5	11.42 ± 1.4	13.73 ± 1.4
10	30.45 ± 2.1	25.53 ± 2.6
11	12.93 ± 1.5	9.54 ± 0.7
12	20.51 ± 2.3	18.16 ± 1.1

[a] IC_{50} (μM): 1–10 (very strong), 11–20 (strong), 21–50 (moderate), 51–100 (weak), above 100 (non-cytotoxic). [b] Results are means ± S.D. (standard deviation, $n = 3$). [c] According to ref. 42.

These findings indicate that significant potency was achieved *via* conjugation of the parent thiophene core with imide and nitrobenzylidine linkages.[33,43] Also, the enhanced potency of substrates **11** (bearing nitro group) and **12** (bearing phthalimido core) may be attributable for the significant effect of the electron-withdrawing group which improves the ability to inhibit cancer cell proliferation and forming hydrogen bonding with the nucleobases of DNA and causes damage.[34]

Molecular docking study

A molecular docking study of a chemical inhibitor in the active pocket of proper target is widely applied as an approach to disclose the possible antitumor mechanism of action. Microtubules, with diverse roles within the cell, are cellular polymers including chromosomal segregation, cytokine, and chemokine secretion, protein trafficking, maintenance of cell structure, cell migration, and division. A tubulin inhibitor is a drug that inhibits mitosis or cell division and is used in treating cancer. Thus, cancer cells are more sensitive to inhibition of mitosis than normal cells. Therefore, targeting tubulin dynamics is a promising attempt for new chemotherapeutic agents. Substances capable of disturbing microtubules by either stabilizing or destabilizing them would exhibit antiproliferative effects *via* enhancing mitotic arrest and cell apoptosis. At least three main binding sites in tubulin protein, including colchicine, taxane, and vinca alkaloid, have been recognized as targets for the anticancer drugs.[18,23,24] Examples of mitotic inhibitors frequently used in the treatment of cancer include paclitaxel, docetaxel, vinblastine, vincristine, and vinorelbine.

Noteworthy, the promising cytotoxic candidates **5**, **11**, and **12** are tetrahydrobenzo[*b*]thiophenes with diacetyl, Schiff base, and phthalimido functionalities, where these structural units were found to inhibit tubulin polymerization leading to irreversible damage to the tumor vasculature and causes mitotic arrest and tumor necrosis.[44,45] Therefore, the inhibitory potentials of these candidates against tubulin (TUB) domain were investigated *via* molecular docking analysis utilizing molecular

Table 2 Docking results and binding amino acids with compounds **5**, **11**, and **12** to tubulin protein active sites

Compd	*S*-Score (kcal mol^{-1})	RMSD (Å)	Binding amino acids	Interacting groups	Receptor	Type of interaction	Bond length (Å)
5	−6.5483	1.0374	ASN 101	O 25	N	H–acceptor	2.95
			ASN 101	O 25	ND2	H–acceptor	2.87
			GLY 146	N 42	N	H–acceptor	3.39
11	−6.2768	1.6047	ASN 228	C 26	OD1	H–donor	3.25
			ASP 69	6-Ring	OD2	Pi–H	3.32
			ASN 101	6-Ring	ND2	Pi–H	3.55
			ASN 101	6-Ring	N	Pi–H	4.31
12	−5.7105	1.6102	GLN 11	O 30	NE2	H–acceptor	2.73
			SER 178	O 31	OG	H–acceptor	2.98
			ASN 101	6-Ring	ND2	Pi–H	3.33
Paclitaxel	−8.9669	1.8961	SER 178	O 32	O	H–donor	2.79
			GLN 11	O 51	OE1	H–donor	2.91
Co-crystallized ligand (GTP)	−11.9309	1.4869					

Table 3 2D and 3D-interactions of substances **5**, **11**, and **12** with tubulin protein binding pockets

Compd	2D	3D
5	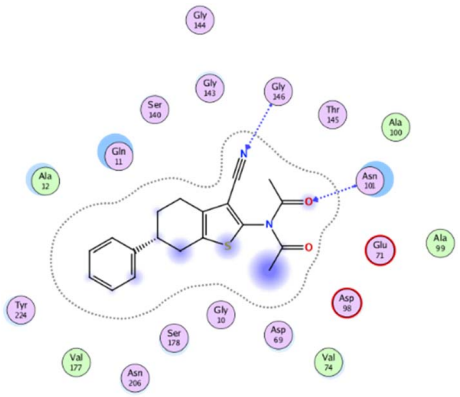	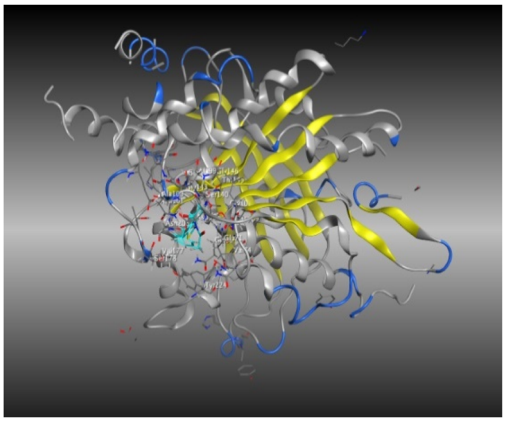
11	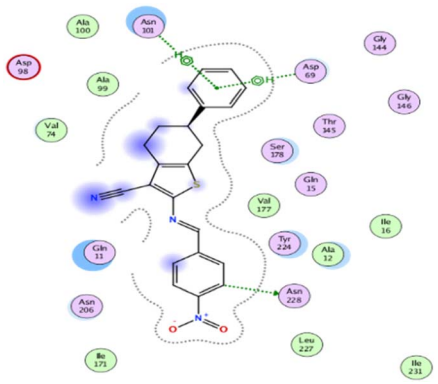	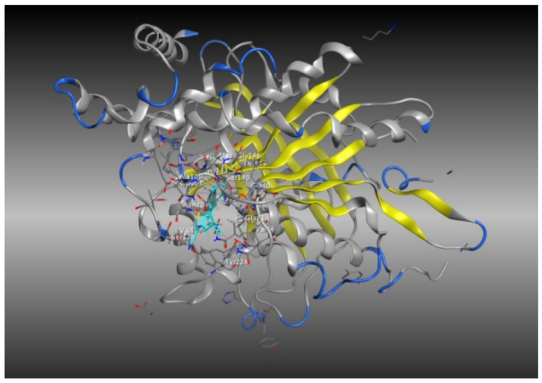
12	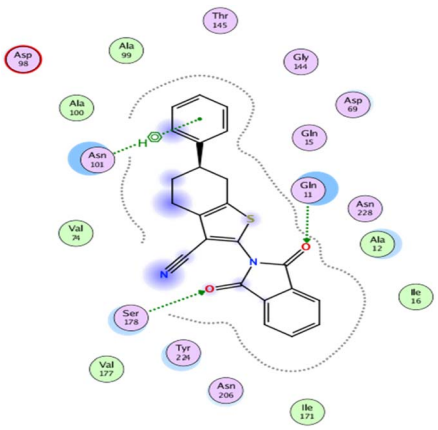	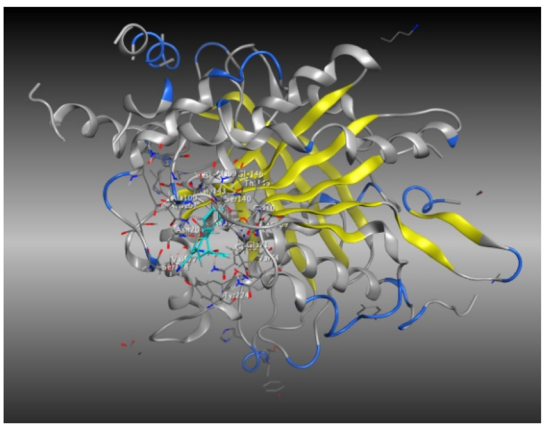
Paclitaxel	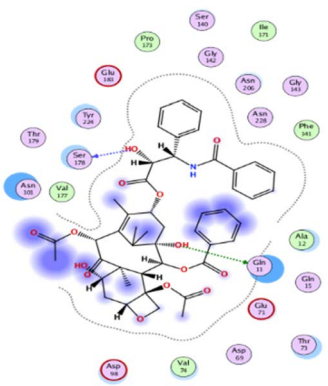	

Table 3 (*Contd.*)

Compd	2D	3D
Co-crystallized ligand (GTP)	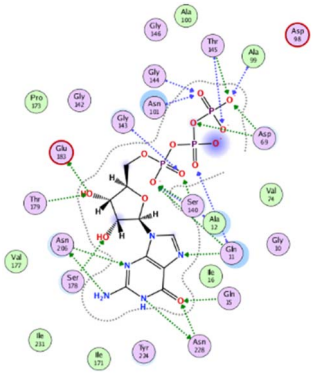	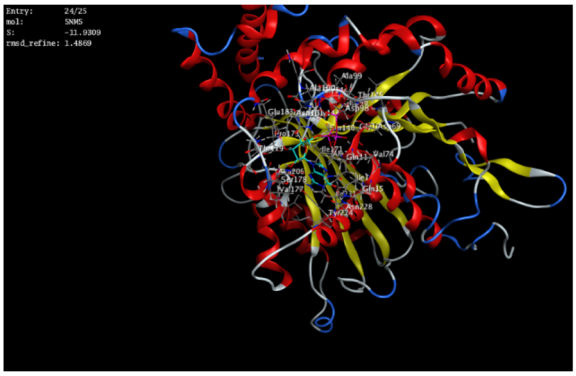

operating environment (MOE 2014.0901) to disclose its probable antitumor mechanism of action, examine the binding free energies of the prepared substances and paclitaxel (as a tubulin stabilizing agent) toward tubulin protein (PDB ID 5NM5) and display the interactions between the prepared ligands and receptors.

The binding affinities were measured by the binding energies (*S*-score, kcal mol^{-1}) and hydrogen bonds. All complexes obtained were docked in the same groove of binding site of the native co-crystallized ligand (GTP) (Tables 2 and 3). Further, Table 2 mentions the specific amino acids involved in binding interactions between each compound and its respective target protein through inclusive information concerning the binding amino acids and types of bonds formed like H–acceptor, pi–cation, and among others.

The data presented in Table 2 revealed that the binding energies of the synthesized ligands were near to that of co-crystallized ligand (GTP) with RMSD values lower than 2 Å. Noteworthy, the co-crystallized ligand (GTP) and paclitaxel exhibited binding energies of −11.9309 and −8.9669 kcal mol^{-1} with RMSD values of 1.8961 and 1.4869 Å, respectively. The inhibition efficiency of paclitaxel was attributed to the hydrogen bonding interaction with some amino acids (SER 178 and GLN 11) of tubulin protein. The best docking score was displayed by compound **5** as it showed binding energy of −6.5483 kcal mol^{-1} with the lowest RMSD of 1.0374 Å indicating to its tightly hydrogen bonding to some key nucleobases and amino acids (ASN 101, GLY 146) of tubulin protein, which disclose its potential utilization as tubulin stabilizing agents like paclitaxel. Also, compounds **11** and **12** exhibited binding energies of −6.2768 and −5.7105 kcal mol^{-1} with RMSD of 1.6047 and 1.6102 Å, respectively, which display notably strong binding affinities toward tubulin protein through hydrogen bonding and pi–hydrogen interactions. The orientation and hydrogen bond pattern of these compounds in the active sites correspond to that of paclitaxel, as a tubulin stabilizing agent.

The outcomes of docking analysis of compounds **5**, **11**, and **12** with the tubulin protein (PDB ID 5NM5) were displayed in graphical representations designated as 2D and 3D visualizations (*cf.* Table 3). The 3D visualization displays the binding interactions between these substances and tubulin protein, indicating hydrogen bonding interactions highlighted in red. Also, 2D depiction illustrates detailed insights into the molecular interactions between compounds and proteins.

Modeling pharmacokinetics

The ADME (absorption, distribution, metabolism, and excretion) properties of the compelling substances, which involve their physicochemical properties, lipophilicity, and drug-likeness, have been prophesied by SwissADME free web tool to lessen the time of choosing substrates from an enormous collection of substances in the early phases of drug discovery, biological effects, and development for an effective drug.[18,46] Compounds **5**, **11**, and **12** were found to obey with Lipinski's rule of five with a total polar surface area (TPSA) of 89.41, 110.21, and 89.41 Å, respectively (*cf.* Table S2 and Fig. S2–S12 in ESI†).[12,47]

Also, these substances displayed suitable physicochemical properties, which was examined through the following six parameters: lipophilicity (LIPO), size, polarity (POLAR), insolubility (INSOL), unsaturation (UNSAT), and flexibility (FLEX). Concerning the absorption property, they displayed gastrointestinal tract (GIT) absorption due to their existence in the BOILED-EGG chart white area (Fig. S13 in ESI†). They showed good lipophilicity as presented by the consensus log $P_{o/w}$ which were in 3.45, 4.39, and 4.37, respectively. The good oral bioavailability (0.55) of these substances was clear through the bioavailability radar chart. Thus, compounds **5**, **11**, and **12** were fully included in the pink area and this supported their well-predicted oral bioavailability. They showed a high GI absorption. Their skin permeation (log K_P) parameters were −5.94, −4.83, and −5.23 cm s^{-1}, which rendered the bioactive compounds easier to access through skin. Also, their cytochrome P450 isoenzymes (CYP1A2, CYP2C9, CYP2C19, CYP2D6, and CYP3A4), which perform a significant role in biotransformation of medicines through O-type oxidation processes, have

also been estimated. In turn, it is expected to penetrate the blood–brain barrier (existed inside the chart yellow area). Further, they are not potential substrates for permeability glycoprotein (PGP), which is indicated by red. Finally, all compounds showed no violations to Lipinski's rule of five except for compound **8** as displayed in Table S2 (ESI†). Jointly, compounds **5**, **11**, and **12** exhibit desirable drug-likeness and oral bioavailability properties.

Conclusion

Certain tetrahydrobenzo[*b*]thiophene candidates were prepared starting from the corresponding β-enaminonitrile scaffold. The *in vitro* antiproliferative activity of the examined substances against MCF7 and HePG2 cell lines displayed the relative highest potency of imide **5**, Schiff base **11**, and phthalimido **12** compared with doxorubicin and paclitaxel. The DFT results were coherent with the cytotoxicity of tested compounds by displaying the lowest ΔE values of 1.540, 1.976, and 6.090 eV and highest softness of 1.299, 1.012, and 1.013 eV^{-1} for compounds **11**, **12**, and **5**, respectively, compared with other compounds. A molecular docking study was performed employing MOE to investigate the binding free energies of paclitaxel (as a tubulin inhibitor) and potent substrates toward tubulin protein (PDB ID 5NM5) and determined the interactions between ligands obtained and receptors. The binding energies of ligands obtained were near to that of co-crystallized ligand (GTP). The best docking score was given by imide derivative **5** (-6.5483 kcal mol^{-1}) indicating its tightly bounding through hydrogen bonding with some key nucleobases and amino acids (ASN 101 and GLY 146) of tubulin protein and revealing its potential utility as tubulin inhibitor. Also, compounds **11** and **12** showed notably strong binding affinity towards tubulin protein. A modeling pharmacokinetics study of all prepared compounds showed that substances **5**, **11**, and **12** were fully included in the pink area supporting their well-predicted oral bioavailability. The most potent candidates may serve as useful lead substrates in looking for selective and powerful antiproliferative agents.

Materials and methods

All solvents and reagents were purified and dried employing standard approaches. The melting points of all substances were taken on a GRIFFIN and GEORGE melting-point apparatus. Infrared (IR) spectra (ν, cm^{-1}) were determined at a NICOLET iS10 infrared spectrophotometer employing KBr disks. ^{1}H and ^{13}C NMR spectra (δ, ppm) were acquired at 400 and 100 MHz, respectively on a Bruker Avance III NMR spectrometer employing deuterated dimethyl sulfoxide (DMSO-d_6) solvent with tetramethyl silane (TMS) internal standard. Mass spectra were run on a Shimadzu GC-MSQP-1000 EX mass spectrometer (Thermo Scientific GCMS MODEL (ISQ LT)) running at 70 eV using the Thermo X-CALIBUR software at Regional Center for Mycology and Biotechnology (RCMB), Al-Azhar University, Cairo, Egypt. Elemental analyses were recorded at a CHN analyzer, and values obtained were within ±0.4 of the theoretical values. The homogeneity of the substances obtained was controlled by TLC (thin-layer chromatography) on plates with employing aluminum sheet silica gel 60 F254 (Merck, Darmstadt, Germany) with different solvent systems as mobile phases.

2-Amino-6-phenyl-4,5,6,7-tetrahydrobenzo[*b*]thiophene-3-carbonitrile (2)

To a solution of 4-phenylcyclohexanone (5.22 g, 30 mmol), malononitrile (1.98 g, 30 mmol) and elemental sulfur (0.96 g, 30 mmol) in methyl alcohol (10 mL), diethylamine (2 mL) was added dropwise with stirring at 50–60 °C for 10 min. Then heating for 1 h at the same temperature. The solution was allowed to stand at room temperature and the solid formed was filtered off, washed with ethanol several times, dried, and crystallized from ethanol to give beige crystals, mp 181–182 °C [lit. [35] mp 180–182 °C], yield (5.64 g, 74%).

N-(3-Cyano-6-phenyl-4,5,6,7-tetrahydrobenzo[*b*]thiophen-2-yl) acetamide (3)

A solution of β-enaminonitrile **2** (1.27 g, 5 mmol) in ethanoic anhydride (10 mL) or glacial ethanoic acid (10 mL) involving fused sodium acetate (2 g) was refluxed for 1 h. The formed solid after cooling was collected and crystallized from ethyl alcohol to obtain white crystals, mp 234–235 °C, yield (1.27 g, 86%). R_f = 0.41 (Et_2O/EtOAc, 2 : 1). IR (ν, cm^{-1}): 3265 (NH), 2216 (C≡N), 1695 (C=O). ^{1}H NMR (δ, ppm): 1.87–1.93 (m, 2H, CH_2), 2.19 (s, 3H, CH_3), 2.62–2.71 (m, 2H, CH_2), 2.83–2.88 (m, 2H, CH_2), 2.93–2.99 (m, 1H, CH), 7.22 (t, 1H, Ar–H, J = 7.5 Hz), 7.29–7.34 (m, 4H, Ar–H), 11.57 (br.s, 1H, NH, exchangeable). EIMS, m/z (%): 296.09 ($M^{+\bullet}$, 12), 268.11 (14), 229.09 (20), 228.07 (100), 227.04 (61), 211.09 (5), 194.09 (6), 155.07 (15), 140.06 (21), 119.05 (15), 93.08 (27), 77.07 (55), 65.07 (22). Anal. calcd for $C_{17}H_{16}N_2OS$ (296.39): C, 68.89; H, 5.44; N, 9.45; found: C, 68.79; H, 5.38; N, 9.43%.

2-Methyl-7-phenyl-5,6,7,8-tetrahydrobenzo[4,5]thieno[2,3-*d*] pyrimidin-4(3*H*)-one (4)

A solution of **2** (1.27 g, 5 mmol) in ethanoic anhydride (10 mL) was refluxed for 6 h. The formed solid after cooling was collected and crystallized from 1,4-dioxane to obtain white crystals, mp > 300 °C, yield (1.20 g, 81%). R_f = 0.45 (Et_2O/EtOAc, 3 : 1). IR (ν, cm^{-1}): 3200 (NH), 1669 (C=O). ^{13}C NMR (δ, ppm): 163.35, 158.53, 154.43, 145.59, 130.45 (2), 130.19, 128.42 (2), 126.87, 126.31, 119.95, 38.82, 32.05, 29.15, 25.61, 20.82. ^{1}H NMR (δ, ppm): 1.91–2.01 (m, 2H, CH_2), 2.33 (s, 3H, CH_3), 2.80–2.87 (m, 2H, CH_2), 2.96–3.03 (m, 2H, CH_2), 3.11–3.15 (m, 1H, CH), 7.23 (t, 1H, Ar–H, J = 7.4 Hz), 7.32–7.33 (m, 4H, Ar–H), 12.25 (br.s, 1H, NH, exchangeable). Anal. calcd for $C_{17}H_{16}N_2OS$ (296.39): C, 68.89; H, 5.44; N, 9.45; found: C, 68.80; H, 5.39; N, 9.47%.

Action of ethanoic anhydride or ethanoic/sulfuric acids on acetamide derivative 3

A solution of acetamide derivative **3** (1.48 g, 5 mmol) in ethanoic anhydride (10 mL) or ethanoic acid (10 mL) containing

concentrated sulfuric acid (0.1 mL) was refluxed for 2–3 h. After cooling, the reaction mixture was poured onto cold-water to get a mixture of heteroannulated product **4** and imide derivative **5** which was filtered off, dried, and fractionally recrystallized from ethyl alcohol to obtain the imide derivative **5**. The insoluble residue was recrystallized from dioxane to achieve hetero-annulated product **4** (identity: mp, mixed mp, TLC), yield (0.59 g, 40%).

N-Acetyl-*N*-(3-cyano-6-phenyl-4,5,6,7-tetrahydrobenzo[*b*]thiophen-2-yl)acetamide (5)

White crystals, mp > 300 °C, yield (0.91 g, 54%). $R_f = 0.52$ (Et_2O/EtOAc, 3 : 1). IR (ν, cm^{-1}): 2219 (C≡N), 1737, 1712 (C=O vibrational coupling). ^1H NMR (δ, ppm): 1.95–2.07 (m, 2H, CH_2), 2.34 (s, 6H, 2 CH_3), 2.64–2.78 (m, 2H, CH_2), 2.82–2.89 (m, 2H, CH_2), 3.03–3.08 (m, 1H, CH), 7.24 (t, 1H, Ar–H, $J = 7.5$ Hz), 7.31–7.35 (m, 4H, Ar–H). EIMS, m/z (%): 338.31 ($M^{+\cdot}$, 12), 306.32 (37), 283.40 (100), 228.20 (41), 200.30 (32), 172.21 (17), 132.36 (21), 98.52 (35). Anal. calcd for $C_{19}H_{18}N_2O_2S$ (338.43): C, 67.43; H, 5.36; N, 8.28; found: C, 67.32; H, 5.29; N, 8.31%.

N-(3-Cyano-6-phenyl-4,5,6,7-tetrahydrobenzo[*b*]thiophen-2-yl) formamide (6)

A solution of **2** (1.27 g, 5 mmol) in formic acid (10 mL) was refluxed for 30 min. The formed solid was collected, washed well with water, dried, and crystallized from ethanol to offer white crystals, mp 251–253 °C, yield (1.27 g, 90%). $R_f = 0.48$ (Et_2O/EtOAc, 3 : 1). IR (ν, cm^{-1}): 3185 (NH), 2212 (C≡N), 1684 (C=O). ^1H NMR (δ, ppm): 1.58–1.80 (m, 2H, CH_2), 1.99–2.22 (m, 2H, CH_2), 2.74–2.84 (m, 2H, CH_2), 2.95–3.06 (m, 1H, CH), 7.21–7.28 (m, 4H, Ar–H), 7.36 (t, 1H, Ar–H, $J = 7.4$ Hz), 8.50 (s, 1H, CHO), 8.67 (br.s, 1H, NH, exchangeable). Anal. calcd for $C_{16}H_{14}N_2OS$ (282.36): C, 68.06; H, 5.00; N, 9.92; found: C, 67.99; H, 4.96; N, 9.94%.

7-Phenyl-5,6,7,8-tetrahydrobenzo[4,5]thieno[2,3-*d*]pyrimidin-4(3*H*)-one (7)

A solution of **2** (1.27 g, 5 mmol) in formic acid (10 mL) was refluxed for 3 h. The excess solvent was evaporated under vacuum. The residue was triturated with light petroleum, filtered, and recrystallized from 1,4-dioxane/DMF mixture (2 : 1) to get white crystals, mp >360 °C, yield (1.07 g, 76%). $R_f = 0.46$ (Et_2O/EtOAc, 3 : 1). IR (ν, cm^{-1}): 3190 (NH), 1659 (C=O). ^1H NMR (δ, ppm): 1.96–2.07 (m, 2H, CH_2), 2.74–2.89 (m, 2H, CH_2), 3.00–3.14 (m, 2H, CH_2), 3.35–3.57 (m, 1H, CH), 7.23 (t, 1H, Ar–H, $J = 7.3$ Hz), 7.32–7.40 (m, 4H, Ar–H), 8.02 (s, 1H, CH=N), 12.34 (br.s, 1H, NH, exchangeable). Anal. calcd for $C_{16}H_{14}N_2OS$ (282.36): C, 68.06; H, 5.00; N, 9.92; found: C, 67.95; H, 4.94; N, 9.95%.

N^1,N^4-Bis(3-cyano-6-phenyl-4,5,6,7-tetrahydrobenzo[*b*]thiophen-2-yl)terephthalamide (8)

To a stirred solution of **2** (1.27 g, 5 mmol) in 1,4-dioxane (15 mL) containing triethylamine (0.1 mL), terephthaloyl dichloride (0.51 g, 2.5 mmol) was added portion wise. The reaction mixture was further stirred for 5 h at ambient temperature. The solid obtained was collected and recrystallized from 1,4-dioxane to produce beige crystals, mp >300 °C, yield (2.87 g, 90%). $R_f = 0.56$ (Et_2O/EtOAc, 1 : 1). IR (ν, cm^{-1}): 3235 (NH), 2223 (C≡N), 1664 (C=O). ^1H NMR (δ, ppm): 1.17–1.23 (m, 4H, 2CH_2), 1.95–2.05 (m, 4H, 2CH_2), 2.70–2.81 (m, 4H, 2CH_2), 2.94–3.17 (m, 2H, 2CH), 7.22–7.43 (m, 10H, Ar–H), 8.04–8.13 (m, 4H, Ar–H), 11.97 (br.s, 2H, 2NH, exchangeable). Anal. cald. for $C_{38}H_{30}N_4O_2S_2$ (638.80): C, 71.45; H, 4.73; N, 8.77; found: C, 71.32; H, 4.65; N, 8.80%.

7-Phenyl-5,6,7,8-tetrahydrobenzo[4,5]thieno[2,3-*d*]pyrimidin-4-amine (9)

A solution of **2** (1.27 g, 5 mmol) in formamide (10 mL) was refluxed for 3 h. The solid obtained during reflux was filtered and recrystallized from 1,4-dioxane to get colorless crystals, mp 252–253 °C, yield (1.15 g, 82%). $R_f = 0.38$ (Et_2O/EtOAc, 2 : 1). IR (ν, cm^{-1}): 3285, 3200 (NH_2), 1636 (C=N). ^{13}C NMR (δ, ppm): 158.19, 153.09 (2), 145.54, 130.61 (3), 128.50 (3), 126.97, 126.45, 40.38, 32.48, 29.38, 25.83. ^1H NMR (δ, ppm): 1.98–2.05 (m, 2H, CH_2), 2.87–2.99 (m, 2H, CH_2), 3.01–3.10 (m, 2H, CH_2), 3.37–3.55 (m, 1H, CH), 6.84 (br.s, 2H, NH_2, exchangeable), 7.23 (t, 1H, Ar–H, $J = 7.4$ Hz), 7.32–7.41 (m, 4H, Ar–H), 8.20 (s, 1H, CH=N). Anal. calcd for $C_{16}H_{15}N_3S$ (281.38): C, 68.30; H, 5.37; N, 14.93; found: C, 68.20; H, 5.32; N, 14.95%.

7-Phenyl-5,6,7,8-tetrahydrobenzo[4,5]thieno[2,3-*d*]pyrimidine-2,4(1*H*,3*H*)-dithione (10)

A mixture of **2** (1.27 g, 5 mmol) and carbon disulfide (10 mL) in pyridine or alcoholic potassium hydroxide (10%, 10 mL) was heated at 65–75 °C for 8 h on water bath. The solution was poured onto crushed ice/cold-water and acidified with diluted hydrochloric acid (10%). The formed solid was filtered, washed well with water, dried, and crystallized from ethanol/1,4-dioxane mixture (2 : 1) to give pale-yellow crystals, mp >300 °C, yield (1.40 g, 85%) and (1.25 g, 76%), respectively. $R_f = 0.43$ (Et_2O/EtOAc, 1 : 1). IR (ν, cm^{-1}): 3119 (NH), 1190 (C=S). ^{13}C NMR (δ, ppm): 181.65, 169.22, 149.99, 148.25, 145.50, 129.54, 128.50 (2), 126.99, 126.42 (2), 125.17, 40.39, 32.15, 29.13, 27.91. ^1H NMR (δ, ppm): 1.85–2.00 (m, 2H, CH_2), 2.74–2.81 (m, 2H, CH_2), 2.81–2.98 (m, 2H, CH_2), 3.02–3.42 (m, 1H, CH), 7.21 (t, 1H, Ar–H, $J = 7.3$ Hz), 7.24–7.32 (m, 4H, Ar–H), 13.22 (br.s, 1H, NHCS, exchangeable), 13.89 (br.s, 1H, NHCS, exchangeable). Anal. calcd for $C_{16}H_{14}N_2S_3$ (330.48): C, 58.15; H, 4.27; N, 8.48; found: C, 58.07; H, 4.21; N, 8.51%.

(*E*/*Z*)-2-((4-Nitrobenzylidene)amino)-6-phenyl-4,5,6,7-tetrahydrobenzo[*b*]thiophene-3-carbonitrile (11)

A mixture of **2** (1.27 g, 5 mmol) and 4-nitrobenzaldehyde (0.75 g, 5 mmol) in glacial ethanoic acid (neat condition) was refluxed for 15 min. The solid formed while refluxing was filtered and recrystallized from 1,4-dioxane/DMF (2 : 1) to give orange crystals, mp >300 °C, yield (1.88 g, 97%). $R_f = 0.47$ (Et_2O/EtOAc, 1 : 1). IR (ν, cm^{-1}): 2218 (C≡N), 1600 (C=N), 1556, 1336 (NO_2). ^1H NMR (δ, ppm): 1.97–2.10 (m, 2H, CH_2), 2.78–2.89 (m, 2H, CH_2), 2.92–3.09 (m, 2H, CH_2), 3.17–3.25 (m, 1H, CH), 7.24 (t, 1H, Ar–

H, $J = 7.2$ Hz), 7.26–7.37 (m, 4H, Ar–H), 8.22 (d, 2H, $-C_6H_4NO_2$, $J = 8.7$ Hz), 8.40 (d, 2H, $-C_6H_4NO_2$, $J = 8.7$ Hz), 8.84 (s, 1H, CH=N). EIMS, *m*/*z* (%): 387.35 ($M^{+\bullet}$, 38), 383.00 (76), 365.46 (26), 364.68 (31), 361.33 (52), 344.67 (93), 338.69 (37), 323.07 (23), 278.75 (35), 252.03 (51), 236.28 (65), 224.91 (47), 216.42 (39), 156.91 (55), 144.09 (57), 133.34 (37), 118.91 (54), 103.15 (31), 96.25 (100), 80.83 (38), 73.99 (51), 67.09 (35). Anal. calcd for $C_{22}H_{17}N_3O_2S$ (387.46): C, 68.20; H, 4.42; N, 10.85; found: C, 68.11; H, 4.36; N, 10.83%.

2-(1,3-Dioxoisoindolin-2-yl)-6-phenyl-4,5,6,7-tetrahydrobenzo[*b*]thiophene-3-carbonitrile (12)

A mixture of **2** (1.27 g, 5 mmol) and phthalic anhydride (0.74 g, 5 mmol) in glacial ethanoic acid (2 mL) was refluxed for 1 h or neat condition. The solid formed during reflux was filtered and recrystallized from ethyl alcohol to get bright-yellow crystals, mp 277–278 °C, yield (1.07 g, 56%). $R_f = 0.53$ (Et_2O/EtOAc, 1 : 1). IR (ν, cm^{-1}): 2225 (C≡N), 1788, 1730 (C=O vibrational coupling). ^1H NMR (δ, ppm): 2.03–2.10 (m, 2H, CH_2), 2.22–2.29 (m, 2H, CH_2), 2.86–2.97 (m, 2H, CH_2), 3.07–3.12 (m, 1H, CH), 7.27-7.32-7.40 (m, 7H, Ar–H), 7.89 (d, 1H, Ar–H, $J = 7.2$ Hz), 8.03 (d, 1H, Ar–H, $J = 7.2$ Hz). EIMS, *m*/*z* (%): 384.31 ($M^{+\bullet}$, 22), 309.06 (3), 284.17 (4), 230.09 (7), 229.09 (20), 228.09 (84), 227.08 (57), 155.09 (30), 140.07 (60), 115.06 (37), 114.08 (34), 89.08 (18), 77.07 (100), 59.01 (96), 51.07 (50). Anal. calcd for $C_{23}H_{16}N_2O_2S$ (384.45): C, 71.86; H, 4.20; N, 7.29; found: C, 71.80; H, 4.16; N, 7.30%.

Conflicts of interest

No potential conflict of interest was reported by the authors.

References

1 S. Higazy, N. Samir, A. El-Khouly, *et al.*, Identification of thienopyrimidine derivatives tethered with sulfonamide and other moieties as carbonic anhydrase inhibitors: design, synthesis and anti-proliferative activity, *Bioorg. Chem.*, 2024, **144**, 107089.

2 A. H. Abadi, T. M. Ibrahim, K. M. Abouzid, *et al.*, Design, synthesis and biological evaluation of novel pyridine derivatives as anticancer agents and phosphodiesterase 3 inhibitors, *Bioorg. Med. Chem.*, 2009, **17**(16), 5974–5982.

3 A. El-Sewedy, E. A. El-Bordany, N. F. Mahmoud, *et al.*, One-pot synthesis, computational chemical study, molecular docking, biological study, and *in silico* prediction ADME/pharmacokinetics properties of 5-substituted 1*H*-tetrazole derivatives, *Sci. Rep.*, 2023, **13**(1), 17869.

4 S. K. Ramadan, D. R. Abdel Haleem, H. S. Abd-Rabboh, *et al.*, Synthesis, SAR studies, and insecticidal activities of certain N-heterocycles derived from 3-((2-chloroquinolin-3-yl) methylene)-5-phenylfuran-2(3*H*)-one against Culex pipiens L. larvae, *RSC Adv.*, 2022, **12**(22), 13628–13638.

5 M. M. Kaddah, A. A. Fahmi, M. M. Kamel, S. A. Rizk and S. K. Ramadan, Rodenticidal Activity of Some Quinoline-Based Heterocycles Derived from Hydrazide-Hydrazone Derivative, *Polycyclic Aromat. Compd.*, 2023, **43**(5), 4231–4241.

6 S. K. Ramadan, H. S. Abd-Rabboh, N. M. Gad, W. S. I. Abou-Elmagd and D. S. Haneen, Synthesis and Characterization of Some Chitosan-Quinoline Nanocomposites as Potential Insecticidal Agents, *Polycyclic Aromat. Compd.*, 2023, **43**(8), 7013–7026.

7 M. A. Aziz, R. A. Serya, D. S. Lasheen, *et al.*, Discovery of potent VEGFR-2 inhibitors based on furopyrimidine and thienopyrimidne scaffolds as cancer targeting agents, *Sci. Rep.*, 2016, **6**(1), 24460.

8 M. Asran, E. A. E. El-Helw, M. E. Azab, S. K. Ramadan and M. H. Helal, Synthesis and Antioxidant Activity of Some Benzoquinoline-Based Heterocycles Derived from 2-((3-Chlorobenzo[f]quinolin-2-yl)methylene)hydrazine-1-carbothioamide, *J. Iran. Chem. Soc.*, 2023, **20**(12), 3023–3032.

9 E. A. E. El-Helw, A. Y. Alzahrani and S. K. Ramadan, Synthesis and antimicrobial activity of thiophene-based heterocycles derived from thiophene-2-carbohydrazide, *Future Med. Chem.*, 2024, **16**(5), 439–451.

10 C. J. Shishoo and K. S. Jain, Synthesis of some novel azido/tetrazolothienopyrimidines and their reduction to 2,4-diaminothieno[2,3-*d*]pyrimidines, *J. Heterocycl. Chem.*, 1992, **29**, 883–893.

11 S. K. Ramadan, N. A. Ibrahim, S. A. El-Kaed and E. A. E. El-Helw, New potential fungicides pyrazole-based heterocycles derived from 2-cyano-3-(1,3-diphenyl-1*H*-pyrazol-4-yl) acryloyl isothiocyanate, *J. Sulfur Chem.*, 2021, **42**(5), 529–546.

12 A. S. Elgubbi, E. A. E. El-Helw, A. Y. Alzahrani and S. K. Ramadan, Synthesis, computational chemical study, antiproliferative activity screening, and molecular docking of some thiophene-based oxadiazole, triazole, and thiazolidinone derivatives, *RSC Adv.*, 2024, **14**(9), 5926–5940.

13 A. Archna, S. Pathania and P. A. Chawla, *Bioorg. Chem.*, 2020, **101**, 104026.

14 P. Kavaliauskas, B. Grybaite, M. V. ickevicius, *et al.*, Synthesis, ADMET properties, and *in vitro* antimicrobial and antibiofilm activity of 5-nitro-2-thiophenecarbaldehyde N-((E)-(5-nitrothienyl) methylidene) hydrazone (KTU-286) against *Staphylococcus aureus* with defined resistance mechanisms, *Antibiotics*, 2020, **9**, 612.

15 K. A. El-Sharkawy, H. M. El-Sehrawi and R. A. Ibrahim, The Reaction of 2-Amino-4,5,6,7-tetrahydrobenzo[*b*]thiophenes with Benzoyl-Isothiocyanate: Synthesis of Annulated Thiophene Derivatives and Their Antitumor Evaluations, *Int. J. Org. Chem.*, 2012, **2**(2), 126–134.

16 C. K. Khatri, K. S. Indalkar, C. R. Patil, S. N. Goyal and G. U. Chaturbhuj, Novel 2-phenyl-4,5,6,7-tetrahydro[*b*] benzothiophene analogues as selective COX-2 inhibitors: design, synthesis, anti-inflammatory evaluation, and molecular docking studies, *Bioorg. Med. Chem. Lett.*, 2017, **27**, 1721–1726.

17 R. M. Mohareb and F. M. Manhi, Reaction of Ethyl 2-Diazo-4,5,6,7-tetrahydrobenzo[*b*]thiophene-3-carboxylate with 3-Iminobutyronitrile: Synthesis of Pyridazines, Thiophenes, and Their Fused Derivatives, *Heteroat. Chem.*, 2000, **11**(6), 403–412.

18 S. Kamal, H. A. Derbala, S. S. Alterary, A. B. Bacha, M. Alonazi, M. K. El-Ashrey and N. N. E. El-Sayed, Synthesis, Biological, and Molecular Docking Studies on 4,5,6,7-Tetrahydrobenzo[*b*]thiophene Derivatives and Their Nanoparticles Targeting Colorectal Cancer, *ACS Omega*, 2021, **6**, 28992–29008.

19 Q. Han, Z. Yin, J. Sui, Q. Wang and Y. Sun, A Microwave-Enhanced Synthesis and Biological Evaluation of *N*-Aryl-5,6,7,8-tetrahydrobenzo[4,5]thieno[2,3-*d*]pyrimidin-4-amines, *J. Braz. Chem. Soc.*, 2019, **30**, 1483–1497.

20 M. F. Mohamed, Y. M. Attia, S. A. Shouman and I. A. Abdelhamid, Anticancer activities of new N-Hetaryl-2-Cyanoacetamide derivatives incorporating 4,5,6,7-Tetrahydrobenzo[*b*]Thiophene moiety, *Anti-Cancer Agents Med. Chem.*, 2017, **17**, 1084–1092.

21 R. Elrayess, Y. M. Abdel Aziz, M. S. Elgawish, M. Elewa, A. S. Yassen, S. S. Elhady, H. A. Elshihawy and M. M. Said, Discovery of Potent Dual EGFR/HER2 Inhibitors Based on Thiophene Scaffold Targeting H1299 Lung Cancer Cell Line, *Pharmaceuticals*, 2021, **14**, 9.

22 F. M. Sroor, M. M. Aboelenin, K. F. Mahrous, K. Mahmoud, A. H. M. Elwahy and I. A. Abdelhamid, Novel 2-cyanoacrylamido-4,5,6,7-tetrahydrobenzo[*b*]thiophene derivatives as potent anticancer agents, *Arch. Pharm.*, 2020, **353**, 2000069.

23 T. Weinert, N. Olieric, R. Cheng, *et al.*, Serial millisecond crystallography for routine room-temperature structure determination at synchrotrons, *Nat. Commun.*, 2017, **8**, 542.

24 W. Li, Y. Yin, W. Shuai, F. Xu, H. Yao, J. Liu, K. Cheng, J. Xu, Z. Zhu and S. Xu, Discovery of novel quinazolines as potential anti-tubulin agents occupying three zones of colchicine domain, *Bioorg. Chem.*, 2019, **83**, 380–390.

25 A. M. Abdelrahman, A. A. Fahmi, S. A. Rizk and E. A. E. El-Helw, Synthesis, DFT and Antitumor Activity Screening of Some New Heterocycles Derived from 2,2′-(2-(1,3-Diphenyl-1*H*-pyrazol-4-yl)ethene-1,1-diyl)bis(4*H*-benzo[*d*][1,3]oxazin-4-one), *Polycyclic Aromat. Compd.*, 2023, **43**(1), 721–739.

26 M. M. Kaddah, A. R. Morsy, A. A. Fahmi, *et al.*, Synthesis and biological activity on IBD virus of diverse heterocyclic systems derived from 2-cyano-*N*′-((2-oxo-1,2-dihydroquinolin-3-yl)methylene)acetohydrazide, *Synth. Commun.*, 2021, **51**(22), 3366–3378.

27 A. I. Hassaballah, S. K. Ramadan, S. A. Rizk, E. A. E. El-Helw and S. S. Abdelwahab, Ultrasonic Promoted Regioselective Reactions of the Novel Spiro 3,1-Benzoxazon-Isobenzofuranone Dye Toward Some Organic Base Reagents, *Polycyclic Aromat. Compd.*, 2023, **43**(4), 2973–2989.

28 E. A. E. El-Helw, A. M. Abdelrahman, A. A. Fahmi and S. A. Rizk, Synthesis, Density Functional Theory, Insecticidal Activity, and Molecular Docking of Some N-Heterocycles Derived from 2-((1,3-Diphenyl-1*H*-pyrazol-4-yl) methylene)malonyl diisothiocyanate, *Polycyclic Aromat. Compd.*, 2023, **43**(9), 8265–8281.

29 Y. M. Youssef, M. E. Azab, G. A. Elsayed, A. A. El-Sayed and E. A. E. El-Helw, Synthesis and Antiproliferative Screening of Some Heterocycles Derived from 4-((5-Chloro-3-methyl-1-phenyl-1*H*-pyrazol-4-yl)methylene)-2-phenyloxazol-5(4*H*)-one, *Polycyclic Aromat. Compd.*, 2023, **43**(8), 7152–7163.

30 H. A. Khatab, S. F. Hammad, E. M. El-Fakharany, A. I. Hashem and E. A. E. El-Helw, Synthesis and cytotoxicity evaluation of novel 1,8-acridinedione derivatives bearing phthalimide moiety as potential antitumor agents, *Sci. Rep.*, 2023, **13**(1), 15093.

31 A. M. Abdelrahman, A. A. Fahmi, E. A. E. El-Helw and S. A. Rizk, Facile Synthesis, Biological Evaluation, DFT Studies and *in Silico* Prediction ADME/Pharmacokinetics Properties of *N*-(1-(2-Chlorobenzo[h]quinolin-3-yl)-1-substituted-vin-2-yl)benzamide Derivatives, *Polycyclic Aromat. Compd.*, 2023, **43**(7), 6597–6614.

32 A. M. Youssef, A. K. El-Ziaty, W. S. I. Abou-Elmagd and S. K. Ramadan, Novel Synthesis of Some Imidazolyl-, Benzoxazinyl-, and Quinazolinyl-2,4-dioxothiazolidine Derivatives, *J. Heterocycl. Chem.*, 2015, **52**(1), 278–283.

33 C. H. Tseng, *et al.*, Discovery of 2-[2-(5-nitrofuran-2-yl)vinyl] quinoline derivatives as a novel type of antimetastatic agents, *Bioorg. Med. Chem.*, 2015, **23**(1), 141.

34 K. Miura, T. Oohashi, S. Matsuda and Y. Igarashi, Chemical and Chemotherapeutical Studies on the Furan Derivatives. XXX. Syntheses and Antibacterial Activities of 2-(5-Nitro-2-furyl)vinyl Heterocyclics, *Yakugaku Zasshi*, 1963, **83**, 771–777.

35 Z. Puterová, A. Krutošíková and D. Végh, Gewald reaction: synthesis, properties and applications of substituted 2-aminothiophenes, *ARKIVOC*, 2010, **2010**, 209.

36 F. Akman and N. Çankaya, A study of experimental and theoretical analysis of N-cyclohexylmethacrylamide monomer based on DFT and HF computations, *Pigm. Resin Technol.*, 2016, **45**(5), 301–307.

37 F. Akman, Experimental and theoretical investigation of molecular structure, vibrational analysis, chemical reactivity, electrostatic potential of benzyl methacrylate monomer and homopolymer, *Can. J. Phys.*, 2016, **94**(9), 853–864.

38 K. N. Halim, S. A. Rizk, M. A. El-Hashash and S. K. Ramadan, Straightforward synthesis, antiproliferative screening and density functional theory study of some pyrazolylpyrimidine derivatives, *J. Heterocycl. Chem.*, 2021, **58**(2), 636–645.

39 E. A. E. El-Helw, M. Asran, M. E. Azab, M. H. Helal and S. K. Ramadan, Synthesis, Cytotoxic, and Antioxidant Activity of Some Benzoquinoline-Based Heterocycles, *Polycyclic Aromat. Compd.*, 2023, DOI: **10.1080/10406638.2023.2270767**.

40 M. Jabbari and A. Jabbari, Antioxidant potential and DPPH radical scavenging kinetics of water-insoluble flavonoid naringenin in aqueous solution of micelles, *Colloids Surf., A*, 2016, **489**, 392–399.

41 T. Mosmann, Rapid colorimetric assay for cellular growth and survival: application to proliferation and cytotoxic assay, *J. Immunol. Methods*, 1983, **65**, 55.

42 J. E. Liebmann, J. A. Cook, C. Lipschultz, D. Teague, J. Fisher and J. B. Mitchell, Cytotoxic studies of paclitaxel (Taxol®) in human tumour cell lines, *Br. J. Cancer*, 1993, **68**, 1104–1109.

43 S. K. Ramadan, H. S. Abd-Rabboh, A. A. Hafez and W. S. I. Abou-Elmagd, Some pyrimidohexahydroquinoline candidates: synthesis, DFT, cytotoxic activity evaluation, molecular docking, and *in silico* studies, *RSC Adv.*, 2024, **14**(23), 16584.
44 R. S. Herbst and F. R. Khuri, Mode of action of docetaxel-a basis for combination with novel anticancer agents, *Cancer Treat. Rev.*, 2003, **29**, 407–415.
45 R. S. Keri, K. Chand, S. Budagumpi, S. B. Somappa, S. A. Patil, B. M. Nagaraja, *et al.*, An overview of benzo[*b*] thiophene based medicinal chemistry, *Eur. J. Med. Chem.*, 2017, **138**, 1002–1033.
46 A. Daina, O. Michielin and V. Zoete, *Sci. Rep.*, 2017, **7**, 42717.
47 C. A. Lipinski, Lead-and drug-like compounds: the rule-of-five revolution, *Drug Discovery Today: Technol.*, 2004, **1**, 337–341.